

$N_\pi = (2.5 \pm 1.1) \times 10^{-4}$ for the decay branch.

The most recent attempt to measure $N_{\gamma\gamma}/N_\pi$ was the work of Alburger and Parker.³ They observed γ - γ coincidences only with no coincidence requirement on the particles and their quoted upper limit is 1.1×10^{-4} , somewhat below our number. However, it does not appear that the two are significantly conflicting.

Several calculations have been attempted to predict two-photon decay branching ratios. In a recent calculation, Bertsch⁷ used a model of the states with spherical and deformed components and evaluated the matrix elements employing the dipole sum rule. Agreement was found with the reported measurement of Beardsworth *et al.*² His revised number⁸ of 3×10^{-4} for ^{16}O is also in good agreement with our results.

In conclusion, this appears to be the first measurement of two-photon emission in $0^+ \rightarrow 0^+$ nuclear transitions free of contaminating or interfering effects. The events attributed to two-pho-

ton decay display the expected characteristics and no alternative explanation for these events is viable.

*Research supported by Lockheed Independent Research Fund.

¹J. C. Vanderleeden and P. S. Jastram, Phys. Rev. C **1**, 1025 (1970); P. Harihar, J. D. Ullman, and C. S. Wu, Phys. Rev. C **2**, 462 (1970); Y. Nakayama, Phys. Rev. C **7**, 322 (1973); Y. Asano and C. S. Wu, Nucl. Phys. A**215**, 557 (1973), and references cited therein.

²E. Beardsworth, R. Hensler, J. W. Tape, N. Bencher-Koller, W. Darcey, and Jack R. McDonald, Phys. Rev. C **8**, 216 (1973).

³D. E. Alburger and P. D. Parker, Phys. Rev. **135**, B294 (1964).

⁴G. Sutter, Ann. Phys. (Paris) **8**, 323 (1963).

⁵D. H. Wilkinson, D. E. Alburger, and J. Lowe, Phys. Rev. **173**, 995 (1968).

⁶W. Heitler, *The Quantum Theory of Radiation* (Oxford Univ. Press, Oxford, England, 1954), p. 384ff.

⁷G. F. Bertsch, Part. Nucl. **4**, 237 (1972).

⁸G. F. Bertsch, private communication.

Hot Spots in Laser Plasmas

R. S. Craxton* and M. G. Haines

Department of Physics, Imperial College, London SW7 2BZ, England

(Received 21 July 1975)

Spontaneously generated magnetic fields can substantially reduce the thermal conductivity in pellet atmospheres and give rise to localized hot spots, which may lead to the ablation of anomalously fast ions.

Magnetic fields have been observed in laser-target experiments and are believed to be thermoelectrically generated as a result of nonparallel density and temperature gradients in the absorption region.¹ In laser-fusion experiments they may grow through a lack of spherical symmetry in the laser irradiation, as is considered in this paper, or from instabilities in an otherwise uniform illumination.²

The electron thermal conduction, essential for the efficient transfer of heat into the compression region, may be drastically reduced by the large value of $\Omega\tau$ generated; this may give rise to "hot spots"—regions where heat is deposited by the laser but prevented from escaping by large confining magnetic fields. By virtue of ion acceleration in the large associated electric fields, these hot spots may be the origin of the suprathermal fast ions observed to carry away

an anomalous proportion of the absorbed energy in ablative kinetic energy. Three other mechanisms are possible: (1) The magnetic fields generated in the absorption region and convected outwards may cause substantial acceleration of the lower-density plasma through the $\vec{J} \times \vec{B}$ force. Although in our simulations the magnetic pressure is generally lower than the plasma pressure we do not rule out this effect on longer time scales. (2) Flux-limited electron thermal conduction (to within a few percent of the free-streaming limit³) may increase the temperature in the absorption region without requiring lack of spherical symmetry. The authors of Ref. 3 mention $\Omega\tau$ effects as an alternative flux-limiting process,⁴ which appears very plausible because of the dependence of conductivity on the square of $\Omega\tau$. (3) Suprathermal electrons, generated where the effect on the local average tem-

perature is small, may convect to a lower-density region, causing a substantial increase in the average temperature there, resulting in ion acceleration to the corresponding energy, again without requiring asymmetry.

A two-dimensional Eulerian code has been developed which focuses attention on the generation of magnetic fields, the electron temperature distribution, and their effect on each other. We describe the model used and a typical run.

If many separate laser beams irradiate a spherical target, local intensity maxima can occur. We consider a region centered on one beam and extending to a boundary of symmetry, equidistant from this beam and neighboring beams, across which all fluxes are zero. We approximate this by taking a Nd-glass laser beam incident from large z along the axis of a cylindrical simulation region, defined by $0 \leq r \leq r_{\max} = 300 \mu\text{m}$ and $0 \leq z \leq z_{\max} = 220 \mu\text{m}$, $r = r_{\max}$ being this boundary of symmetry (at which radial velocity and magnetic field are zero). Zero flux is imposed on $z = 0$, the center of the pellet, while

free flux is allowed on $z = z_{\max}$. The laser beam has a Gaussian radial profile of half-width $0.5r_{\max}$; its power increases linearly to a maximum of 2×10^{12} W at 40 psec, when the peak intensity is 4×10^{15} W/cm², and the peak deposition rate almost 10^{18} W/cm³. A small proportion of the energy is absorbed by inverse bremsstrahlung up to the critical density where the remainder is dumped over the next few mesh points. An initial deuterium plasma of arbitrary temperature 50 eV is assumed; the electron density is a uniform 4×10^{22} cm⁻³ for $0 \leq z \leq 0.25z_{\max}$, drops exponentially through the critical density at $0.5z_{\max}$, to 2.5×10^{19} cm⁻³ at $0.75z_{\max}$, and is uniform for $0.75z_{\max} \leq z \leq z_{\max}$.

We use two-temperature fluid equations for the six variables ρ , T_e , T_i , V_r , V_z , and B_θ , differenced on a 29×41 Eulerian mesh. They include the laser energy dump, electron thermal conduction, the magnetic-field source term, hydrodynamics, $\vec{J} \times \vec{B}$ forces, equipartition, the Hall term, bremsstrahlung loss, inverse bremsstrahlung absorption, ion thermal conduction, magnet-

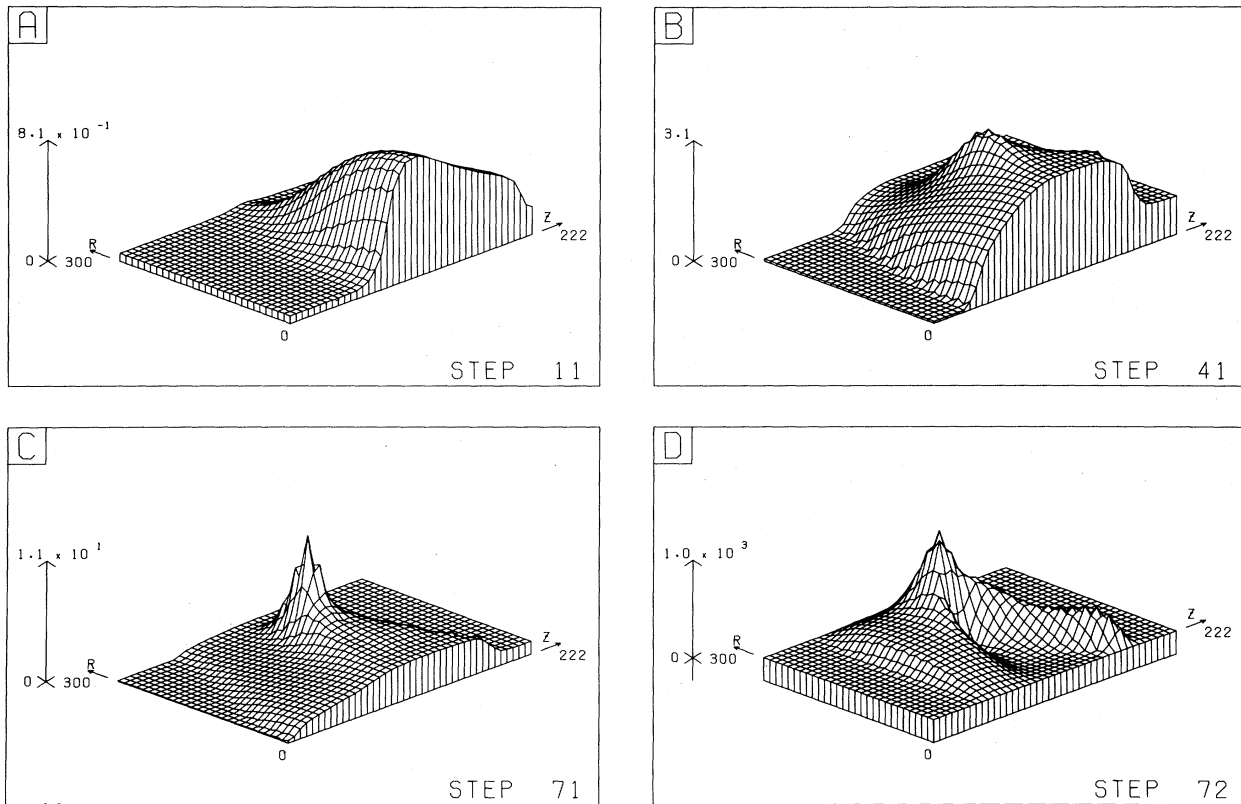


FIG. 1. (a)–(c) Distributions of electron temperature (T_e), in keV, at 6, 35, and 65 psec, respectively. (d) Distribution of azimuthal magnetic field (B), in kG, at 65 psec. The plots are scaled to the maximum, which is indicated by the arrow on the left.

ic field convection, and the perfect-gas equation of state. The first three phenomena dominate, and are associated with picosecond time scales; resistivity, which is unlikely to be important in our parameter regimes, is excluded.

The equation for azimuthal magnetic field is

$$\frac{\partial B_\theta}{\partial t} = \left\{ -\nabla \times \left[-\vec{V}_e \times \vec{B} - \frac{1}{ne} \nabla(nkT_e) \right] \right\}_\theta \quad (1)$$

$$= -\frac{1}{ne} \frac{\partial T_e}{\partial r} \frac{\partial n}{\partial z} + \text{smaller terms}, \quad (2)$$

the source term largely determined by $\partial T_e / \partial r$, and the electron heat flux is given by

$$q_e = -\frac{K_0}{1 + (\Omega\tau)^2} \nabla T_e, \quad (3)$$

where $K_0 = \text{const} T_e^{5/2}$ is the classical conductivity,⁵ Ω the electron Larmor frequency, and τ the electron collision time.

To treat mesh diffusion times $< 10^{-2}$ psec the diffusion terms in the equation for T_e are differenced fully implicitly, and the resulting quin-

diagonal matrix is solved by use of the alternating-direction-implicit iterative method. The hydromagnetics makes use of the two-step Lax-Wendroff method in a section based on the code FOCUS of Potter.⁶

Figure 1(a) shows the distribution of T_e at 6 psec. The laser beam is incident from the right along the z axis; the electron temperature is essentially determined by the local absorption of laser energy and thermal conduction is only effective as yet in the low-density region.

Figure 1(b) shows T_e at 35 psec; we note the thermal front advancing towards the solid, but the dominant feature is the hot spot, with a peak temperature of 3.1 keV. The hot spot always occurs in a region of absorption and large $\Omega\tau$; at this time the maximum values of $\Omega\tau$ and B_θ are 102 and 145 kG, respectively. Figure 1(c) shows T_e at 65 psec; the hot spot is more pronounced, with a peak of 11 keV, and is more distant from the axis.

From (2), B_θ is largely a response to $\partial T_e / \partial r$, so that the source term is reversed on the axial

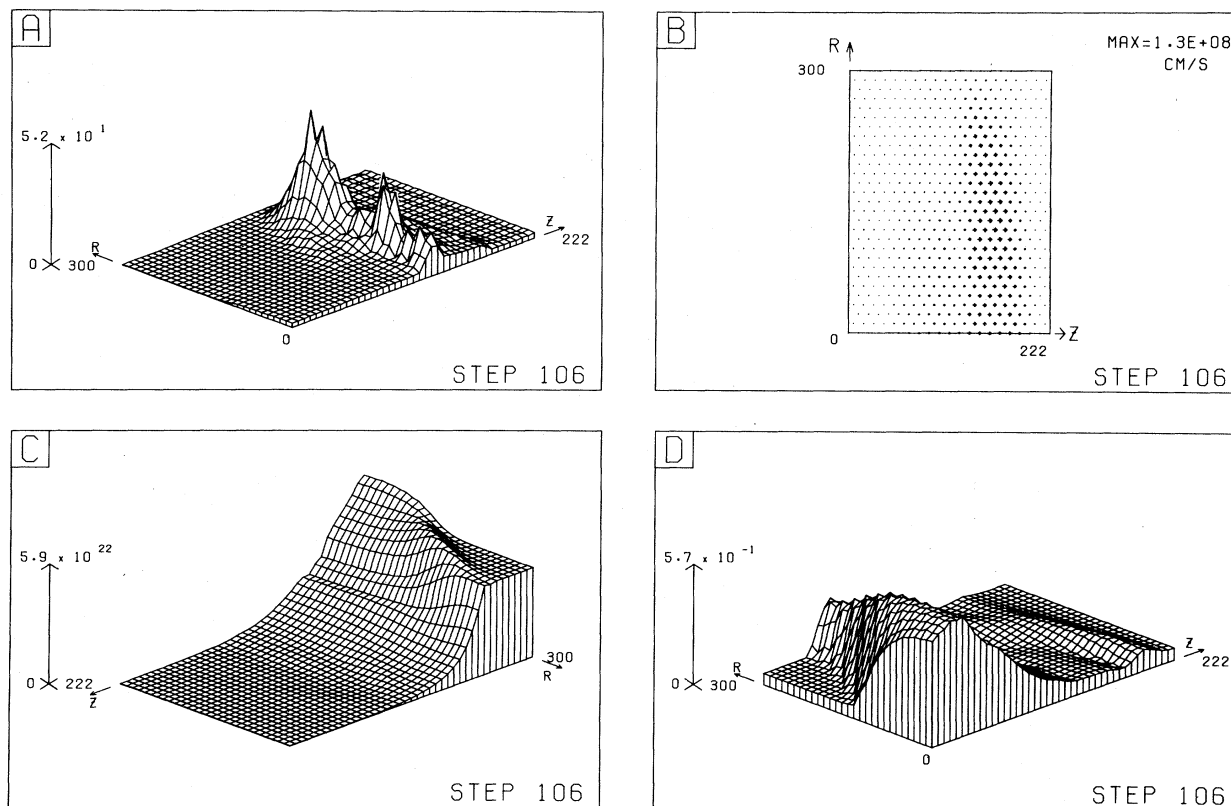


FIG. 2. (a)–(d) Distributions of T_e , in keV, ion velocity in cm/sec, density ρ , in electrons/cm³, and ion temperature T_i , in keV, respectively, at 99 psec.

side of a hot spot but enhanced on the other side. Consequently the region of most restricted conductivity (and therefore the hot spot) gradually moves away from the axis. Figure 1(d) shows the distribution of $-B_\theta$ at 65 psec and illustrates this point. The peak of 1 MG occurs at slightly larger radius than the hot spot. Between the hot spot and the axis are regions of reduced and reversed magnetic field. This implies a conduction path along which $\Omega\tau$ is zero, in addition to the obvious conduction paths at the axis and the "symmetry" boundary $r=r_{\max}$. The peak magnetic field reaches 3 MG at 88 psec and 5 MG at 99 psec.

Figure 2(a) shows T_e at 99 psec. The hot spot peaks at 52 keV, dwarfing by comparison the remainder of the distribution. The structure has fragmented somewhat, with a second hot spot appearing nearer the axis. The two hot spots are each surrounded by large magnetic fields, of opposite signs, and therefore with a conduction path in between. The scale length of this structure is related to the original scale length of the incident laser profile.

The velocity field generated by the pressure gradient is shown in Fig. 2(b) at 99 psec, the peak velocity of 1.3×10^8 cm/sec corresponding to an ion energy of 17 keV. Over all, 79% of laser energy has gone into electron thermal energy, 15% into ion thermal energy (in the denser region), and 6% into kinetic energy of ablation, although the rate of transfer to ablating ions is increasing.

Figure 2(c) shows ρ at 99 psec, viewed from the opposite direction to previous plots. Slight compression is observed, with a peak of 1.4 times the initial solid density. The thermal front has not yet reached the region around $(r, z) = (300 \mu\text{m}, 0)$, whereas if $\Omega\tau$ effects are excluded T_e rapidly diffuses radially and the compression front is uniform over r .

Figure 2(d) shows T_i at 99 psec. Equipartition is effective only in the higher-density and lower-temperature region, while in the hot-spot region large ablative velocities cause expansion and cooling of the ions.

We have performed various other runs, hot spots appearing in most cases. The source term for B_θ [Eq. (2)] may be reduced by choosing a lower density gradient or greater laser spatial

half-width. Initially conduction may be sufficiently effective to produce an almost flat $T(r)$, and only later when $\Omega\tau$ becomes large enough to reduce the conductivity will the hot spot form. A fluctuating radial profile, e.g.,

$$f(r) \propto 1 + 0.5 \cos(2\pi r/r_{\max}), \quad (4)$$

gives rise to two hot spots, originating near $r=0$ and $r=r_{\max}$, and moving towards each other. From Eq. (2) it is clear that a reversed magnetic field configuration is set up, with an $\Omega\tau=0$ conduction path in the middle. We have obtained similar results for a CO₂ laser, although smaller laser intensities are needed to give similar temperatures at similar times because of the lower density of the absorption region. For the same reason $\Omega\tau$ effects are enhanced. Also, we have considered the heat flow perpendicular to the temperature gradient (the Righi-Leduc effect) which presents computational difficulties.

We conclude with a note of caution: These hot spots are driven by a largely assumed energy-absorption mechanism, and while azimuthal magnetic fields may not in themselves inhibit the absorption there must come a temperature beyond which the efficacy of the anomalous mechanisms decreases. Unfortunately this is outside the scope of the present work.

Note added.—Our attention has been drawn to work by D. Colombant *et al.* (to be published). Studying a computer model of x-ray emission from an aluminum target, these authors also find an off-axis maximum of the electron temperature, though less pronounced than here.

*Work supported by Culham Laboratory Agreement CUL/926.

¹J. A. Stamper, K. Papadopoulos, R. N. Sudan, S. O. Dean, E. A. McLean, and J. M. Dawson, *Phys. Rev. Lett.* **26**, 1012 (1971).

²D. A. Tidman and R. A. Shanny, *Phys. Fluids* **17**, 1207 (1974).

³R. C. Malone, R. L. McCrory, and R. L. Morse, *Phys. Rev. Lett.* **34**, 721 (1975).

⁴N. K. Winsor and D. A. Tidman, *Phys. Rev. Lett.* **31**, 1044 (1973).

⁵B. B. Robinson and I. B. Bernstein, *Ann. Phys. (N.Y.)* **18**, 110 (1962).

⁶D. E. Potter, *Phys. Fluids* **14**, 1911 (1971).